Korean J. Chem. Eng., 39(8), 2089-2098 (2022)
DOI: 10.1007/s11814-022-1175-3

pISSN: 0256-1115
eISSN: 1975-7220

Impact of ammonium sulfate and kaolin on ash deposition during co-firing of straw pellets and pulverized coal

Ho Lim*, Yumi Park*, Yongwoon Lee*, Youngjae Lee*, Taeyoung Chae*, Jaewook Lee*,†, Won Yang*,,†, and Jaekwan Kim*,***

*Carbon Neutral Technology R&D Department, Korea Institute of Industrial Technology, 89, Yangdaegiro-gil, Ipjang-myeon, Seobuk-gu, Cheonan-si, Chungchungnam-do 31056, Korea
**Department of Clean Process and System Engineering, University of Science and Technology, 217 Gajeong-ro, Yuseong-gu, Daejeon 34113, Korea
***KEPCO Research Institute, 105 Munji-ro, Yuseong-gu, Daejeon 34056, Korea
(*Received 6 December 2021 • Revised 25 March 2022 • Accepted 11 May 2022*)

Abstract−This study investigated the effects of additives on reduction in ash deposit formation while co-firing straw pellets with pulverized coal. A pulverized-fuel-fired combustion system was used to co-combust sub-bituminous coal and herbaceous biomass. Kaolin ($Al_2Si_2O_5(OH)_4$) and ammonium sulfate ($(NH_4)_2SO_4$) were used to determine the influence of additives on ash deposit reduction. Experiments were performed in an 80 kW_{th} scale combustion system for various proportions of additives (proportions of 1 wt% and 4 wt% of fuel). Weight of deposited ash was measured concurrently. In the experimental results, different trends from several previous researches were observed regarding effectiveness of the additives: Addition of kaolin increased deposition by up to 19%, while ammonium sulfate increased deposition by up to 36%. Thermodynamic equilibrium of all experimental cases was calculated based on ash composition, and we reveal that in our experimental cases kaolin promotes formation of K-silicates of low melting temperature, while ammonium sulfate reacts with KCl to increase melting temperatures for K-Al-silicates. This demonstrates that the fuel-specific choice of additives is important to effectively reduce ash deposition.

Keywords: Additives, Ammonium Sulfate, Ash Deposition, Co-firing, Herbaceous Biomass, Kaolin

INTRODUCTION

Biomass is a renewable energy source that can be utilized in coal-fired power plants in place of a portion of the coal typically used; accordingly, biomass can reduce overall greenhouse gas emissions from coal-fired power plants by reducing CO_2 emissions [1]. Substitution of biomass for coal requires only minor modification of existing coal power plants. Moreover, biomass co-firing offers economic benefits owing to its utilization of abandoned resources such as agricultural byproducts. Korean power plants primarily use wood biomass pellets for co-firing. However, recent policy changes have made it difficult to obtain a renewable energy certificate (REC) for the use of imported wood biomass. This leads to increased use of domestic biomass, including herbaceous one for co-firing in pulverized coal power stations.

Herbaceous biomass differs from woody biomass in terms of ash content and composition. In particular, herbaceous biomass has higher ash content and produces relatively high quantities of ash deposits in boilers, leading to reduced efficiency. Additionally, herbaceous biomass has higher content of chlorine (Cl) and alkali metals such as sodium (Na) and potassium (K) than woody biomass [2]. The alkali metals are vaporized during combustion and form alkali salts of low melting temperature, which causes more ash deposition (slagging and fouling) in boiler tubes. It may interrupt system operations, thus affecting operational stability and resulting in economic loss [2-7].

To address this problem, there are several alternative ways. Parts of them are associated with combustion temperature control; it is necessary to use additives that can convert compounds with low melting temperature into those with high melting temperature. In contrast to other methods that decrease ash deposition, the use of additives is known to be economical and efficient because it does not require modification of the boiler [8]. The basic mechanisms underlying the effects of additive chemical components are shown in Eqs. (1)-(5) [9]. In each chemical reaction, the addition of an additive produces high-temperature molten compounds and thus reduces ash deposition during combustion.

Aluminum silicate-based additives

$$Al_2O_3{\cdot}xSiO_2+2KCl+H_2O \rightarrow K_2O{\cdot}Al_2O_3{\cdot}xSiO_2+2HCl\ (g) \quad (1)$$

Sulfur-based additives

$$SO_2\ (g)+\tfrac{1}{2}O_2\ (g) \rightarrow SO_3\ (g) \quad (2)$$

$$SO_3\ (g)+2KCl\ (g)+H_2O\ (g) \rightarrow 2HCl\ (g)+K_2SO_4 \quad (3)$$

Calcium-based additives

$$K_2O{\cdot}SiO_2+2CaCO_3 \rightarrow 2CaO{\cdot}K_2O{\cdot}SiO_2+2CO_2\ (g) \quad (4)$$

Phosphorus-based additives

$$KCl\ (g)+CaHPO_4{\cdot}2H_2O \rightarrow CaKPO_4+2H_2O+HCl\ (g) \quad (5)$$

†To whom correspondence should be addressed.
E-mail: lee_jw@kitech.re.kr, yangwon@kitech.re.kr

Previous studies have tested several types of additives in boilers and under laboratory conditions to investigate reduction in ash deposition from solid fuel. Additives based on S [10-12], Al-Si [13-15], and P or P-Ca [16,17] can reduce the formation of ash deposits by reacting with KCl, which is the main component responsible for ash deposition in most of Eqs. (1)-(5). Previously, Aho et al. [10] investigated the alkali capture efficiency of aluminum, finding that it decreased ash deposition in a pilot-scale fluidized bed (FB) reactor. Similarly, Kassman et al. [11] reported that elemental sulfur and ammonium sulfate can convert alkali chlorides (mainly KCl) to alkali sulfates, which reduces deposition, in a 12 MW circulating fluidized bed (CFB) boiler. Use of Ca- or Mg-based additives has been shown to convert low-temperature molten compounds (which increase deposition) into high-temperature molten compounds (which decrease deposition) [17]. Broadly, previous studies have demonstrated that the addition of kaolin and ammonium sulfate can reduce deposition [8,11,12,18,19]; however, there is a lack of data regarding the application of additives for different fuels, particularly herbaceous biomass.

The present study investigated the effects of additives on ash deposition during the co-firing of herbaceous biomass with coal. In particular, a co-firing experiment was performed in an 80-kW_{th}-scale combustion system at the Korea Institute of Industrial Technology (KITECH), where herbaceous biomass pellets were co-fired with pulverized coal. During the experiment, the mass of ash deposited was measured in real time for two additives—kaolin ($Al_2Si_2O_5(OH)_4$) and ammonium sulfate ($(NH_4)_2SO_4$). These additives were chosen specifically for this study to observe the impact of ash deposit formation on the co-firing process. Scanning electron microscopy/energy dispersive X-ray spectroscopy (SEM/EDS), X-ray diffraction (XRD) spectroscopy, and inductively coupled plasma (ICP) analyses were performed for the deposits obtained in the pilot experiment using the 80-kW_{th}-scale combustion system. To interpret the experimental results in detail, the amount of liquid slag and chemical composition of ash during combustion for various conditions was simulated using the FactSage7.2 software [20] that calculates thermodynamic chemical equilibrium.

METHODOLOGY

1. Properties of Fuel and Additives

Experiments were performed on a blended fuel comprising 70% Indominco coal, which is sub-bituminous coal, and 30% straw pellets. The fuel properties (ASTM D3176, ASTM D7582-15) and ash compositions (DIN EN 15297:2011 EN) of each component were analyzed based on the standard and are described in Table 1 and Fig. 1, respectively. As shown in Table 1, the biomass component exhibited lower fixed carbon, higher volatile matter, and higher oxygen content than the coal; therefore, the biomass has a comparatively lower heating value. Assuming equal thermal inputs in the co-firing experiment, a greater quantity of biomass must be introduced to achieve the same heating value. Moreover, biomass contains less N than coal, suggesting that NOx emissions will be lower for biomass than coal. However, co-firing is also expected to generate more ash deposition than traditional coal combustion because of the higher ash content of straw pellets.

Table 1. Properties of utilized fuel types

Fuel	Coal	Straw pellet
Ultimate analysis (wt% as received)		
C	65.5	45.4
H	4.3	5.0
O	13.3	33.7
N	1.4	0.6
S	1.3	0.1
Proximate analysis (wt% as received)		
Moisture	9.1	9.2
Volatile matter	43.1	69.7
Fixed carbon	42.7	15.1
Ash	5.1	6.0
Heating value (kcal/kg as dried basis)		
[a]HHV	6,750	4,360
[b]LHV	6,495.7	4,035.8

[a]HHV: Higher Heating Value; [b]LHV: Lower Heating Value

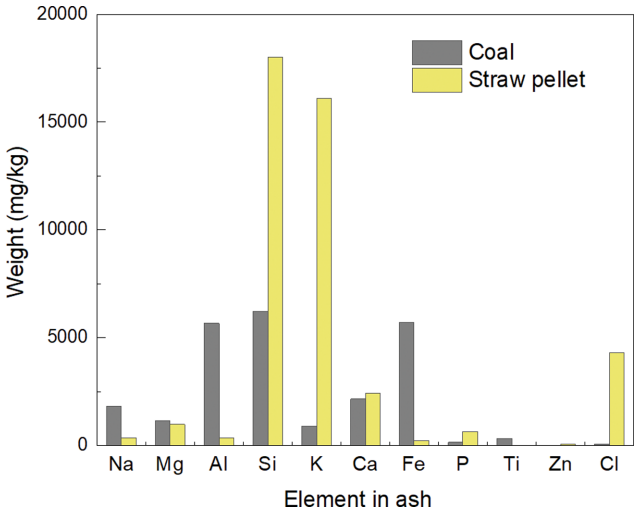

Fig. 1. Element composition of ash of fuels used in this study.

The ash compositions of the two fuels used in this study are shown in Fig. 1; these compositions were determined using an inductively coupled plasma-optical emission spectrometer (ICP-OES). The Cl content of the ash was determined by ion chromatography (IC) analysis. The ICP-OES analysis showed that Ca, K, Si, and Cl, all of which affect ash deposit formation, are more abundant in the straw pellets than in coal. Here, the ash contents of coal and straw pellets were found to be similar, although the elemental composition of the ash was found to vary (Table 1, Fig. 1). Biomass ash is particularly high in Si and K; this impacts deposit formation and suggests that an additive is necessary to reduce deposition. Fig. 2 presents the results of the ash fusion temperature (AFT) analysis. Coal and biomass require different methods of analysis (ASTM D1857). The AFT can be divided into four components for coal: initial deformation temperature (DT), softening temperature (ST), hemispherical temperature (HT), and fluid temperature

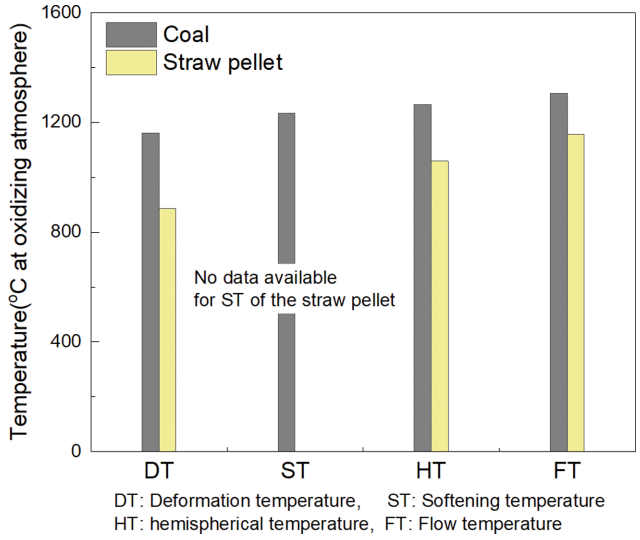

Fig. 2. Ash fusion temperatures of fuels used in this study.

(FT). Here, the ST of biomass was not analyzed owing to differences in analysis methods. The AFT of biomass is lower than that of coal, implying that more deposition should be expected during co-firing than during coal combustion alone [21-23].

The additives used in this study were kaolin ($Al_2Si_2O_5(OH)_4$) and ammonium sulfate ($(NH_4)_2SO_4$), which are typically used to reduce deposition in commercial-scale boilers. These additives were selected to investigate their effects on reducing ash deposition during herbaceous biomass co-firing. The additives were nearly pure compounds (99% purity).

Table 2. Characteristic sizes of the fuels and additives

Cases	Coal	Straw pellet	Ammonium sulfate	Kaolin
d10[a] (μm)	2.3	84.5	159.0	1.2
d50[a] (μm)	8.5	262.0	296.0	9.2
d90[a] (μm)	19.3	476.0	494.0	32.5
Span[b]	2.0	1.5	1.1	3.4

[a]d10, d50, d90: meaning that 10, 50, 90 vol% of the particles is below this size

[b]Span: the width of the distribution defined as (d90−d10)/d50

The particle size distributions of the fuels and additives were determined by a laser diffraction method (Malvern MS3000 laser particle size analyzer). The d50 values of coal, straw pellets, sulfate, and kaolin were found to be approximately 8.5, 262, 296, and 9.2 μm, respectively. The detailed particle size distributions of the fuels and additives are presented in Table 2.

2. Experimental Method and Conditions

Fig. 3 illustrates the 80-kW_{th}-scale combustion system used in this study [24]. The cylindrical furnace has a height of 2,500 mm and internal diameter of 600 mm. The main fuel burner located at the top of the furnace has an 80-kW_{th} tangential vane-type swirl solid fuel burner. Two feeders containing a load cell were installed on top of the burner to feed the coal and biomass separately. The temperature in the furnace wall and gas compositions at the furnace exit were measured with R-type thermocouples and sampling systems connected to gas analyzers. A cyclone was installed behind the burner outlet to collect the heavy fly ash and a bag filter was installed behind the cyclone to collect the light fly ash. A

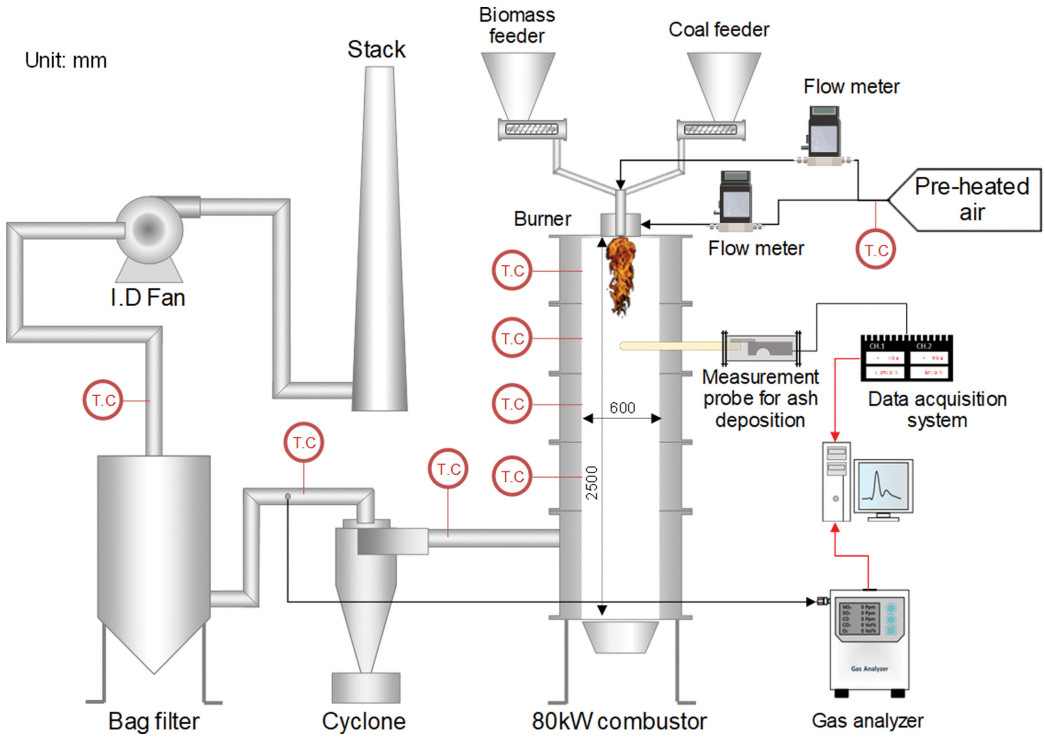

Fig. 3. Schematic diagram of the bench-scale combustion system furnace.

Table 3. Experimental conditions

Fuel type	Coal	Straw Pellet
Feeding rate	8.24 kg/hr	5.70 kg/hr
Thermal input	70% IN+30% SP (thermal input basis) - 80 kW_{th}	
Excess air ratio	0.2	
Additive	Kaolin ($Al_2Si_2O_5(OH)_4$)	Ammonium sulfate ($(NH_4)_2SO_4$)
Amount of additive	1 wt%, 4 wt% (mass basis)	
Experimental time	3 hours	

gas analyzer (ABB 2000) was used to monitor the gas composition (i.e., O_2, CO_2, CO, and NO) at the furnace exit. All temperature and gas composition data were recorded by a data acquisition system. The internal pressure of the furnace was adjusted using an induced draft fan.

As shown Fig. 3, an ash deposit measuring system (ADEMS) was installed 750 mm from the top of the furnace. Deposition on the probe was measured in real time by the load cell and the resulting data were recorded through the data acquisition system. The alumina tube (external diameter: 25 mm) used for the probe was exposed for a minimum of 3 h to allow any deposition trend to be detected. Three methods were adopted to protect the experimental setup from thermal damage: an isolation panel was implemented between the main body and the furnace to screen radiation from the flame; the main body included a water-cooled jacket; and cooling gas was injected into the main body to prevent any temperature increases near load cells. The mass of the deposited ash was determined based on the difference between the mass of the clean probe (measured before the experiment) and the mass of the probe after deposition. This mass was used to verify the real-time deposit weight obtained with the ADEMS. Prior to the experiment, the probe was coated to prevent subsequent detachment of any deposited ash. The elemental composition of the deposited ash was analyzed by SEM/EDS and XRD analyses based on a cross section of the deposited probe. The experimental conditions adopted included a thermal input of 80 kW_{th} and excess air ratio of 0.2. The feeding rate and amount of additive for each fuel are shown in Table 3; co-firing (70% coal, 30% straw pellet) represents the reference case. The portion of straw pellet was selected based on one of the previous researches [25], where maximum 30% for biomass co-firing ratio was applied to pulverized coal combustion system. One recent study [26] shows that 20% is feasible co-firing ratio in the sense of boiler efficiency, but 30% was chosen in this study because it could show effects of co-firing of herbaceous biomass to ash deposition more clearly. Additive amounts were 1 and 4 wt% (by mass) of total fuel feedrates; these proportions are considered appropriate to investigate the correlation between ash deposition behavior and additive proportions based on the experimental variables [27,28]. The additives were blended with straw pellets before being introduced to the furnace.

3. Thermodynamic Chemical Equilibrium Model Calculations

To further analyze the experimental results, thermodynamic chemical equilibrium model calculations were performed using the FactSage7.2 software. FToxide and FTsalt were chosen from the solution database in FactSage 7.2. 'Slag' in the FactSage database is presented as a molten mixture of oxides, while 'Salt' is presented as molten mixtures of alkali salts. The ICP analysis results were used as FactSage input. The calculations were performed for global atmospheric pressure (1 bar) and an excess air ratio of 1.2, same as experi-

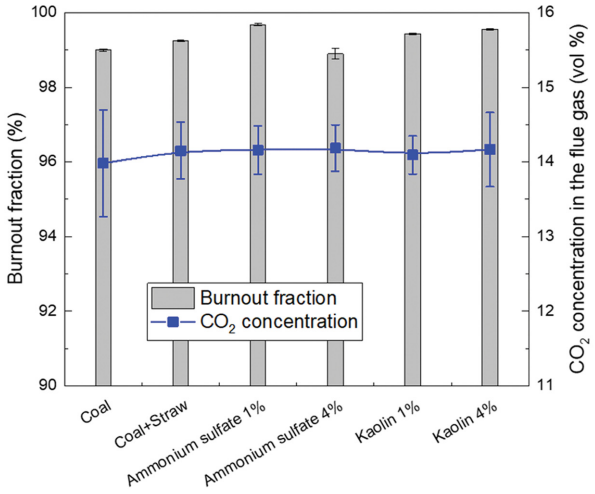

(a) Burnout fraction and CO_2 concentration in the flue gas

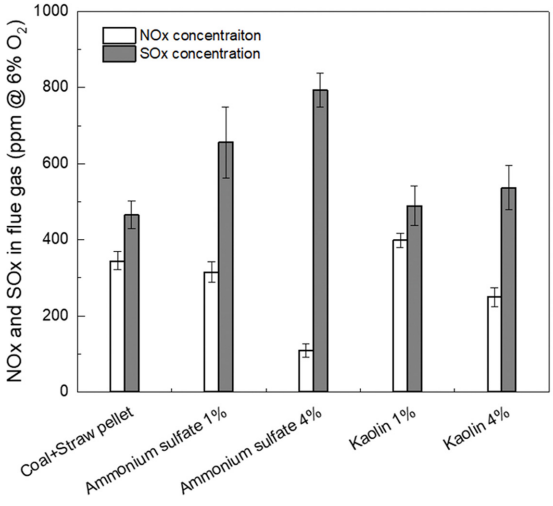

(b) NOx and SOx concentrations in the flue gas

Fig. 4. Burnout fraction and gas concentrations for various additives: (a) Burnout fraction and CO_2 concentration in the flue gas, (b) NO_x and SO_x concentrations.

mental conditions. The calculations were performed for temperatures in the range 800-1,600 °C. From the calculations, the amount of melt and solid phases could be predicted as functions of temperature.

RESULTS AND DISCUSSION

1. Burning Results

The effects of additives on the burning process were considered before investigating deposition. Here, deposition characteristics were evaluated at temperatures greater than ~1,000 °C; at such temperatures, the additives did not cause any differences in the temperature profile.

Fig. 4 illustrates the gas concentration released in flue gas and the burnout fraction in the residue ash. The burnout fraction (%) was calculated according to the ash tracer method [29]. As shown in Fig. 4(a), the burnout fraction was over 99% for all cases considered, and CO_2 concentration was similar for all cases. Fig. 4(b) illustrates NO_X and SO_X concentrations for the experimental cases considered. The gas release pattern remained stable throughout the experiment, except when fuel feeding, with the supply of ammonium sulfate resulting in a slight increase in SO_2 concentration in the flue gas and a relative decrease in NO_X. Compared to the co-firing case without additives, the addition of ammonium sulfate (4 wt%) caused NO_X to decrease by up to 68.6% and SO_X to increase by ~50%. This can be attributed to the decomposition of ammonium sulfate at high temperature and the production of SO_2 (see Eq. (2)). The NH_3 produced by decomposition reacts with NO_X to convert N_2; thus, addition of ammonium sulfate is one of the mechanisms by which NO_X reduction in flue gas occurs. Increases in SO_X can be controlled by a flue gas emission system such as FGD. In contrast to ammonium sulfate, gas release following the addition of kaolin was similar to that for the reference case. Because this additive did not affect combustion, deposition was found to be the same for all experimental cases conducted under the same experimental conditions.

2. Characterization of Ash Deposition

Fig. 5 illustrates the ash deposits that formed on the probe during the experiment. To preserve the deposited ash, the probes were covered by a liquid mixture (resin and hardener) and part of the probe was analyzed by SEM/EDS. Visual observation confirms that different amounts of ash were deposited under different experimental conditions. In particular, ammonium sulfate produced less extensive deposits than kaolin. Some of the material deposited in the ammonium sulfate cases formed a glassy layer that included some ash particles (Fig. 5(c), (d)), whereas bigger particles were formed in the deposits for the kaolin cases (Fig. 5(e), (f)). Therefore, deposition can be considered to have been facilitated by the use of kaolin. The deposition associated with ammonium sulfate seems to present as a relatively thin layer formed by initial deposition of ash particles [30]. In contrast, the deposition associated with other experimental cases indicates more extensive accumulation of ash on the surface. For ammonium sulfate, the glass-like layer developed with increasing exposure time and was difficult to remove. The larger particles associated with the addition of kaolin developed by sintering on the surface, but a glassy layer was also present. Although the sintered layer could be removed easily, the glassy layer could not.

Detailed real-time variation in deposition mass was considered for all cases (Fig. 6); the repeatability of these measurements was confirmed by subsequent methodologically identical experiments. The uncertainty in measurement associated with deposition on the load cell is ±0.2 g, based on material collected after the experiment. Fig. 6 illustrates that the mass of deposition resulting from co-firing of straw pellets was higher than that from coal firing alone; this was to be expected owing to the high potassium content of straw pellets. In this experiment, deposition results depended greatly on the amount and type of additive used, even for identical fuel. For example, total deposition mass decreased by approximately 22% and 36% for addition of 1% and 4% of ammonium sulfate, respectively. Conversely, the addition of 1% and 4% of kaolin increased the deposition mass by approximately 17% and 19%, respectively. These results indicate that different chemical reactions occur depending on the composition of the additive and that fuels containing Si only do not impact deposit formation significantly. How-

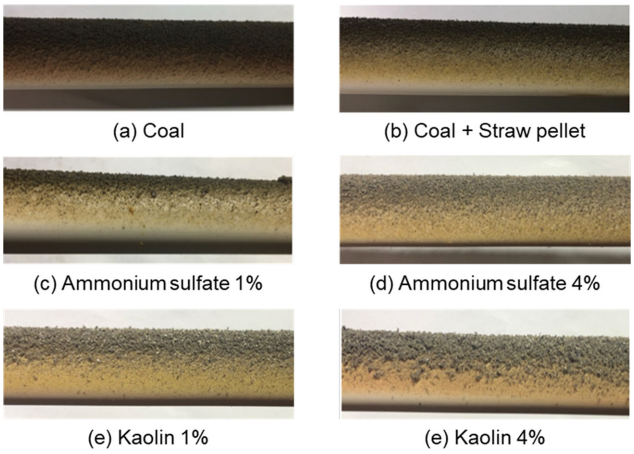

Fig. 5. Photograph of the ash deposit for various kinds and proportion of additives.

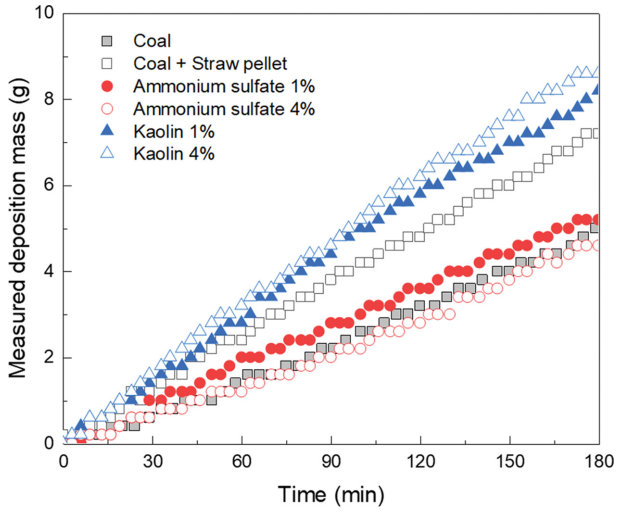

Fig. 6. Real-time measurement results of ash deposition weight for various kinds and proportion of additives.

ever, for fuels containing both K and Si, Si will capture K to form K-silicates. In fact, K-silicates (which have low melting temperatures) and/or K-Al-silicates (which have high melting temperatures) are generated in the reaction between K and Si. In this manner, the formation of compounds with low melting temperature (such as K-silicates) will promote the deposition and accumulation of deposits on the probe surface [16].

The biomass used for co-firing in this study had high Si and K content, and the addition of kaolin-based Si-Al would have accelerated reactions between Si and K. Here, this preferential reaction of Si with K produced K-silicates ($K_2O{\cdot}Al_2O_3{\cdot}xSiO_2$) at the expense of K-Al-silicates for the addition of both 1% and 4% of kaolin.

Deposition propensity [29] was calculated to evaluate the degree of deposition in each experimental case. The following equation was adopted to represent deposition flux.

$$\text{Deposition flux}\left(\frac{\text{g}}{\text{m}^2\cdot\text{hr}}\right)=\left[\frac{\text{Max. deposit rate}\left[\frac{\text{g}}{\text{h}}\right]}{\text{Exposed probe surface}\ [\text{m}^2]}\right] \quad (6)$$

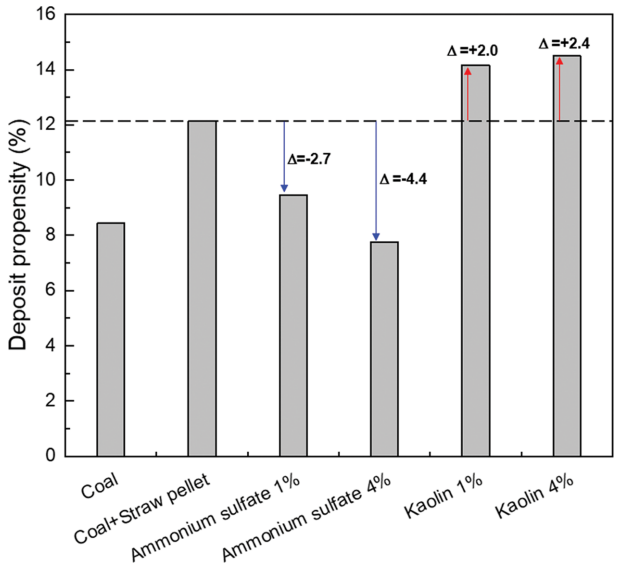

Fig. 7. Deposition propensity various kinds and portion of proportions additives.

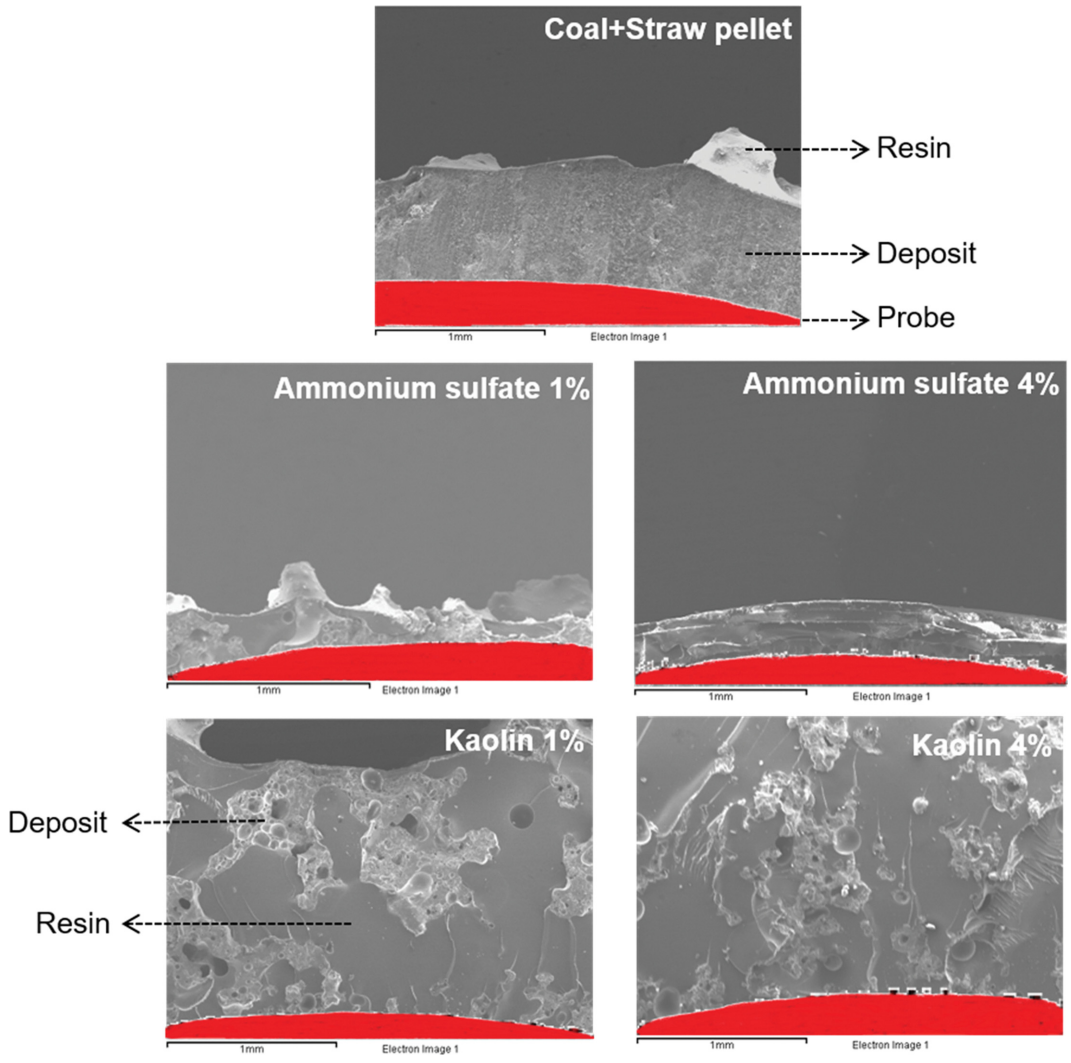

Fig. 8. SEM images of ash deposition on the probe.

The ash flux was determined from the fuel feeding rate, ash ratio, and furnace cross section. In this context, the deposition flux represents the fraction of the input ash flying on the probe. The deposition propensity was calculated as follows.

$$\text{Deposition propensity}\,(\%) = \left[\frac{\text{Deposition flux}\left[\frac{g}{m^2\cdot h}\right]}{\text{Ash flux}\left[\frac{g}{m^2\cdot h}\right]}\right]\times 100 \quad (7)$$

The deposition propensity indicates the ratio of injection of ash to deposition on the probe, as shown in Eq. (7). Thus, this parameter can be used to determine the influence of additives on deposition behavior during co-firing with biomass (Fig. 7). The propensity of ash particles captured by the probe is controlled primarily by the melting temperature and surface distribution and characteristics of the deposits, which are associated with the concentration of alkali silicates present. The results presented here demonstrate that the trend in final deposition weight was similar for all experimental cases (Fig. 6). However, the deposition propensity results help elucidate differences between the experimental cases. In particular, addition of 4% of ammonium sulfate decreased the deposition propensity relative to the co-firing case, while the addition of 4% of kaolin increased the deposition propensity by approximately 2% (Fig. 7).

3. Mineral Element Analysis of Ash Deposits

The morphology of the ash deposits on the probe was characterized by SEM/EDS (Fig. 8). The red part in Fig. 8 represents the aluminum probe, while the white part indicates the mixture used for the coating; some of this mixture has permeated into the deposit layer (shown in dark gray). Ash deposit thickness was lowest for the case with addition of 4% of ammonium sulfate. The SEM/EDS results also indicate that deposition typically presents as two separate parts: particles and agglomerated nucleates. The particles are formed primarily by fragmentation, melting, and coalescence of minerals in the coal, while the nucleates are generated primarily from vaporized inorganic species via vaporization, chemical reac-

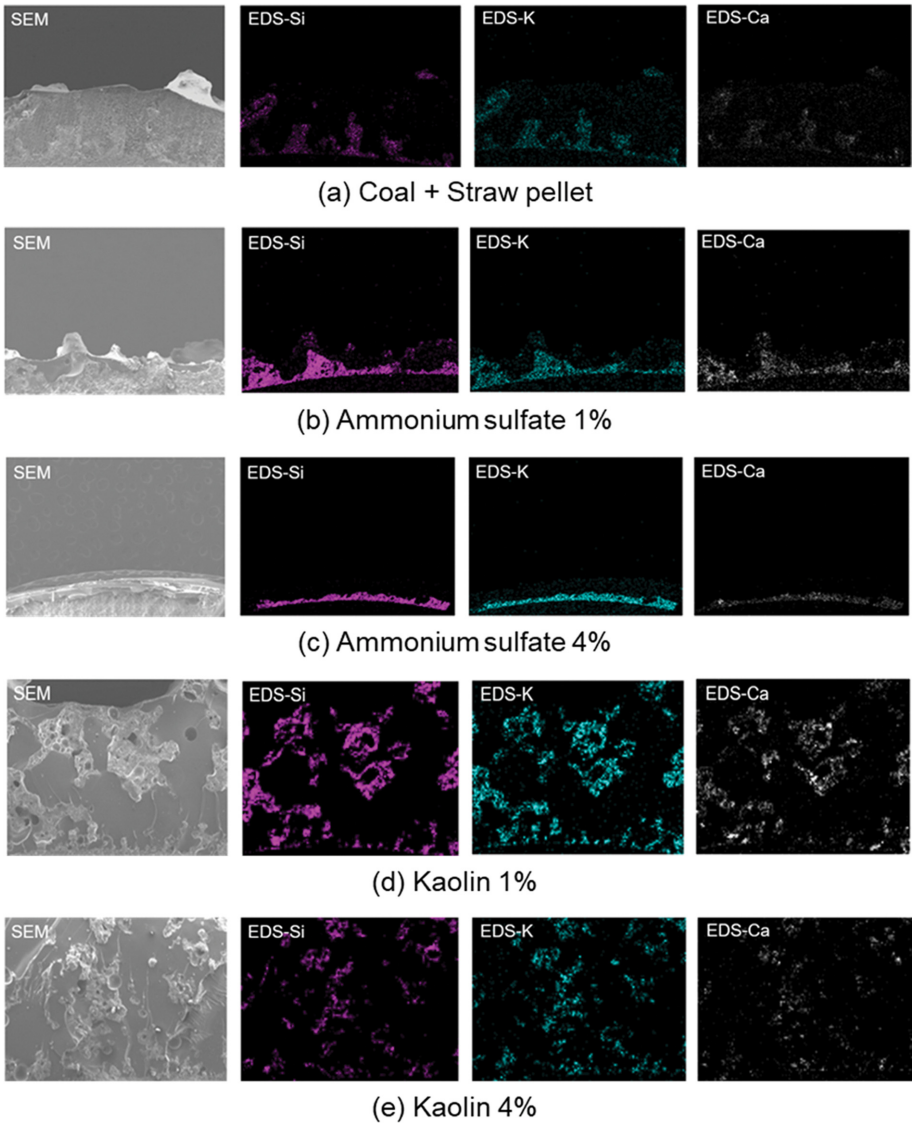

Fig. 9. EDS images of ash deposition on the probe.

tion, nucleation, and coagulation mechanisms [29]. The ammonium sulfate ash exhibits a dense layer of minerals, whereas the kaolin ash has coarse particles interspersed with dense layers [14].

The K-silicates in the deposit layer were observed by EDS analysis. Fig. 9 illustrates the elemental distribution of the deposit layer for each additive. Here, Si, K, and Ca were identified within the same areas, suggesting that these elements are deposited together and control deposit formation. The results demonstrate that more Si, K, and Ca are produced by the addition of kaolin than in other experimental cases. This can be explained with reference to the mechanisms of formation of K- and Ca-silicates. Production of greater quantities of K- and Ca-silicates results in larger deposits.

XRD analysis was conducted to study the mineralogical composition of the deposits. The results, shown in Fig. 10, indicate that the crystallized minerals present are composed primarily of $KAlSi_2O_6$ (cubic-tetragonal crystal structures) in all samples. The addition of additives does not alter the mineralogical composition; however, it does affect the amount of minerals produced. Addition of additives

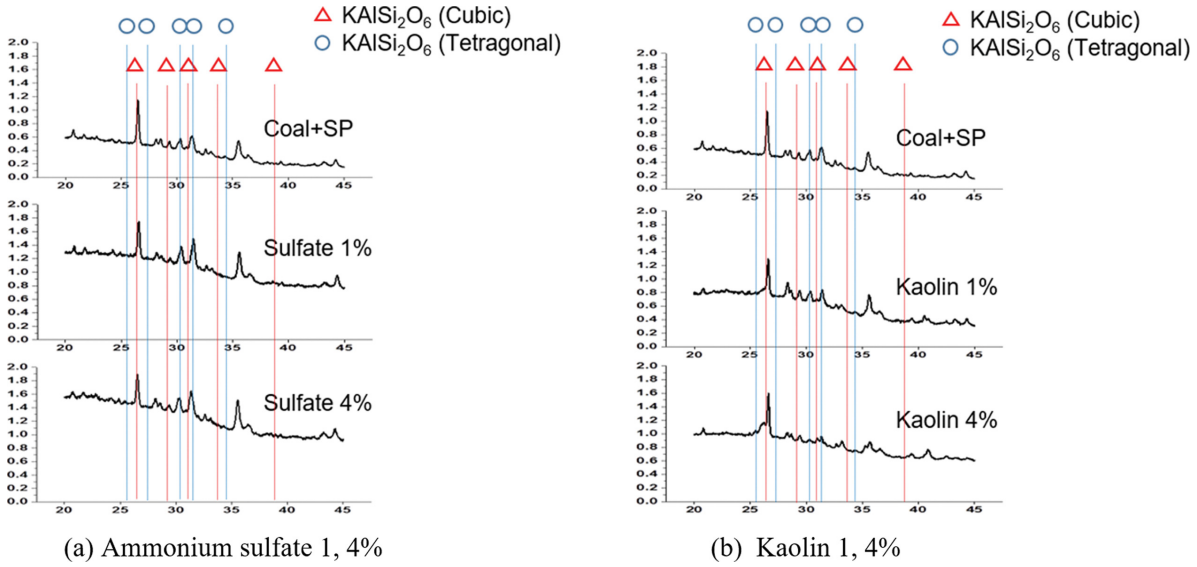

Fig. 10. XRD patterns of deposition depending on experiments.

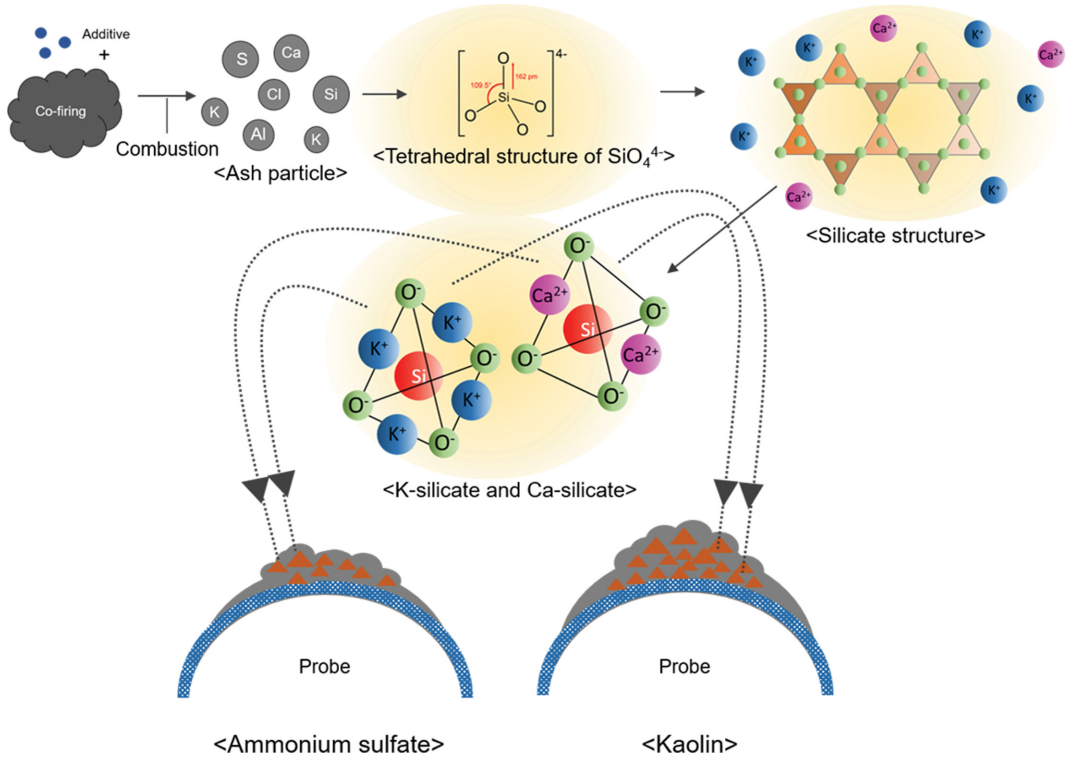

Fig. 11. Mechanism of ash deposition with additives of ammonium sulfate and kaolin.

has been shown to produce $KAlSi_2O_6$, which has a high melting temperature. Here, the addition of kaolin decreased the $KAlSi_2O_6$ peak (relative to the co-firing case without additives), whereas ammonium sulfate increased the $KAlSi_2O_6$ peak. Thus, the addition of kaolin reduced the production of compounds with high melting temperature, thus increasing the amount of material deposited [32].

Fig. 11 illustrates the mechanism of formation of ash deposits for both additives, as determined based on factors including deposit mass and SEM/EDS and XRD results. During co-firing with biomass, various elements in the ash decompose. Here, Si and the alkali metals K and Ca are the major constituents of the ash. The Si contained in the fuel is SiO_4^{4-} oxide, which is very stable and exists on its own, forming a tetrahedral structure. Formation of the tetrahedral structure results in pore generation between the lattices. Ca and K have small atomic size and can exploit these pore spaces because Ca^{2+} and K^+ are cations and are highly reactive with SiO_4^{4-} anions. In this manner, Si captures K and Ca well to form K- and Ca-silicates [14,33,34]. The low melting points of K-silicates and some Ca-silicates promote deposit formation, although the amount produced of such compounds differs depending on the type of additive used. However, the effect of Ca-silicates was not found to be significant in the present study. SO_2 in ammonium sulfate produces SO_3 through oxidation. The SO_3 reacts with K-silicates to form K_2SO_4, a compound that has a high melting temperature and thus does not affect deposit formation. Therefore, the formation of a compound with low melting temperature can be suppressed [10-12]. Conversely, the addition of kaolin (Si-based additive) makes it easier for residual Si to capture alkali metals. Accordingly, the addition of kaolin promotes the production of K-silicates and could enhance deposition.

4. Thermochemical Calculation Results

Thermochemical calculations were performed to predict deposition based on the chemical reactions that occurred between the constituent elements of the fuel and additives. Such calculations can be used to predict the selectivity and efficiency of additives in advance. In the present study, the analysis conditions of the fuels used in the experiment were calculated and the results predicted. Fig. 12 presents the results of the calculations that were undertaken to compare the amount of slag formed as a result of combustion of fuel with/without additives. The calculations were performed at intervals of 200 °C for temperatures of 800-1,600 °C. Kaolin was predicted to produce more slag than combustion without additives, whereas slag formation was predicted to decrease with the addition of ammonium sulfate. These predictions were based on calculations considering various chemical characteristics of the fuels used. Broadly, the calculation results are consistent with the experimental results. However, the addition of ammonium sulfate reduced slag formation by ~4% and 36% based on the calculation results and experimental results, respectively. This discrepancy can be explained by the facts that the equilibrium calculation cannot consider time scale and mixing of additive and fuel cannot be perfect in the experiment. Nevertheless, thermodynamic calculations offer a useful reference method in qualitative ways when chemistry is dominant [35].

Fig. 13 plots in the ternary phase diagram of the SiO_2-Al_2O_3- K_2O system from FactSage. The FTOxide database in FactSage was selected to predict liquidus temperature, proportion of solids. As presented in Fig. 1, SiO_2, Al_2O_3 and K_2O are major ash composition of blended fuel ash and normalized to 100%. According to the proposed reaction mechanisms for the fuels and additives, SiO_2, K_2O, and Al_2O_3 form aluminum alkali silicates with melting temperatures of ~1,500 °C or more when present at a ratio of 1 : 1 : 1. Fig. 13 shows used fuel ash locates the boundary among mullite, Al_2O_3 and $KAlSi_2O_6$. This means blended fuel ash might be a quite sensitivity with additives. When a compound with high melting temperature is produced, the deposit generated by the temperature difference can be reduced. In previous studies, the optimum ratio between fuel and kaolin has been shown to be 1.64 wt%. However, here, the optimum ratio was calculated to be greater than this. This suggests that the fuel used here had high Si and K con-

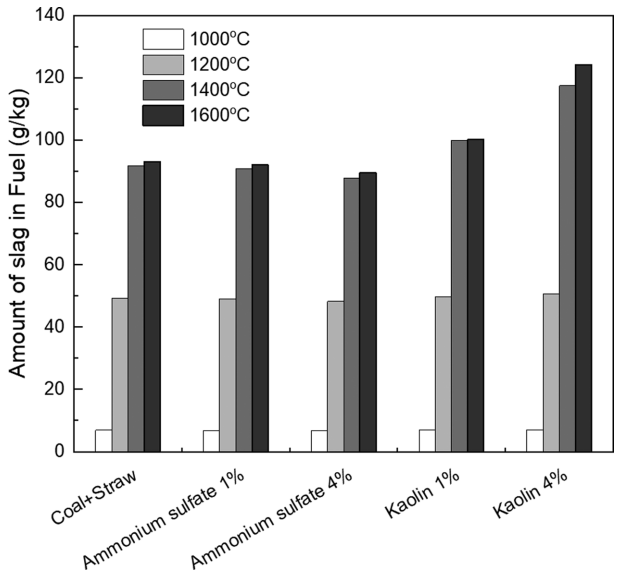

Fig. 12. Difference of slag according to various additives.

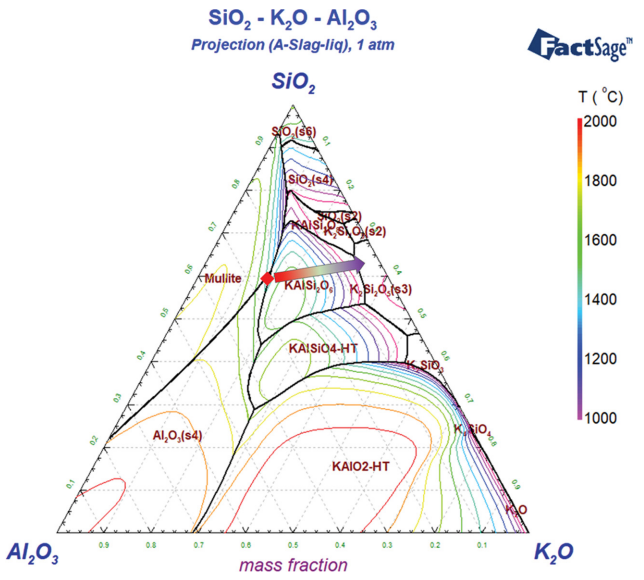

Fig. 13. Phase diagram of SiO_2-Al_2O_3-K_2O.

tent, such that a large amount of Si captured K without reacting at a ratio of 1 : 1, thus forming K-silicates. Compounds without Al have lower melting temperatures, as indicated by the arrow in the phase diagram, and K-silicates are formed below 1,000 °C. In conclusion, deposition mass is higher with the addition of kaolin [27].

CONCLUSIONS

This study investigated the effect of additives on the formation of ash deposition caused by co-firing straw pellets with pulverized coal. Experiments were performed in an 80-kW_{th}-scale pulverized coal combustion system with an ADEMS in real time. Kaolin ($Al_2Si_2O_5(OH)_4$) and ammonium sulfate ($(NH_4)_2SO_4$) were selected as additives. In the results, addition of 1% and 4% of ammonium sulfate decreased the deposition mass by approximately 22% and 36%, respectively. Conversely, addition of 1% and 4% of kaolin increased the deposition mass by approximately 17% and 19%, respectively. When Al-Si-based kaolin was added to the fuel with high potassium and silicate content, residual stable SiO_4^{4-} captured potassium easily and formed greater amounts of K-silicates than in other experimental cases. This occurs because kaolin promotes the formation of K-silicates with low melting temperatures owing to the large amounts of Si and K present in the fuel. In contrast, ammonium sulfate reacts with KCl to cause deposition of ash, containing compounds with high melting temperatures (K-Al-silicates), leading to reduced overall deposition.

This study demonstrates that the effects of additives vary for different fuels; accordingly, optimum additive choice will vary depending on the elemental composition of the fuel used. The results presented here will help improve understanding of fuel characteristics and help ensure the appropriate selection of additives for efficient reduction of ash deposition.

ACKNOWLEDGEMENTS

This study was performed as a part of the R&D project, "Optimization of combustion and flue gas treatment facilities in a coal power generation system for flexible operation" (R20GA10), supported by KEPCO (Korea Electric Power Corporation).

REFERENCES

1. D. Thrän, D. Peetz, K. Schaubach, S. Backéus, L. Benedetti and L. Bruce, Global wood pellet industry and trade study 2017. *IEA Bioenergy Task*, **40** (2017).
2. M. J. Fernández, I. Mediavilla, R. Barro, E. Borjabad, R. Ramos and J. E. Carrasco, *Fuel*, **239**, 1115 (2019).
3. I. Pisa and G. Lazaroiu, *Fuel Process Technol.*, **104**, 356 (2012).
4. B. Sander, *Biomass Bioenergy*, **12**, 177 (1997).
5. K. A. Christensen and H. Livbjerg, *Aerosol Sci. Technol.*, **33**, 470 (2000).
6. M. Öhman, A. Nordin, H. Hedman and R. Jirjis, *Biomass Bioenergy*, **27**, 597 (2004).
7. M. Öhman, C. Boman, H. Hedman, A. Nordin and D. Boström, *Biomass Bioenergy*, **27**, 585 (2004).
8. L. Xu, J. Liu, Y. Kang, Y. Miao, W. Ren and T. Wang, *Energy Fuels*, **28**, 5640 (2014).
9. L. Wang, J. E., Hustad, Ø. Skreiberg, G. Skjevrak and M. Grønli, *Energy Procedia*, **20**, 20 (2012).
10. M. Aho, P. Vainikka, R. Taipale and P. Yrjas, *Fuel*, **87**, 647 (2008).
11. H. Kassman, L. Bäfver and L. E. Åmand, *Combust. Flame,* **157**, 1649 (2010).
12. H. Wu, M. N. Pedersen, J. B. Jespersen, M. Aho, J. Roppo, F. J. Frandsen and P. Glarborg, *Energy Fuels*, **28**, 199 (2014).
13. H. Wu, M. S. Bashir, P. A. Jensen, B. Sander and P. Glarborg, *Fuel*, **113**, 632 (2013).
14. H. Wu, P. Glarborg, F. J. Frandsen, K. Dam-Johansen and P. A. Jensen, *Energy Fuels*, **25**, 2862 (2011).
15. T. K. Gale and J. O. L. Wendt, *Combust Flame*, **131**, 299 (2002).
16. M. S. Bashir, P. A. Jensen, F. Frandsen, S. Wedel, K. Dam-Johansen, J. Wadenbäck and S. T. Pedersen, *Fuel Process Technol.*, **97**, 93 (2012).
17. J. H. Zeuthen, P. A. Jensen and H. Livbjerg, *Energy Fuels*, **21**, 699 (2007).
18. H. Kassman, J. Pettersson, B. M. Steenari and L. E. Åmand, *Fuel Process Technol.*, **105**, 170 (2013).
19. Y. Shao, J. Wang, F. Preto, J. Zhu and C. Xu, *Energies*, **5**, 5171 (2012).
20. C. W. Bale, E. Bélisle, P. Chartrand, S. A. Decterov, G. Eriksson, A. E. Gheribi, K. Hack, I.-H. Jung, Y.-B. Kang, J. Melançon, A. D. Pelton, S. Petersen, C. Robelin, J. Sangster, P. Spencer and M.-A. Van Ende, *Calphad*, **54**, 35 (2016).
21. K. Jagodzińska, W. Gądek, M. Pronobis and S. Kalisz, *IOP Conf. Ser. Earth Environ. Sci.*, **214**, 12080 (2019).
22. Y. Niu, Y. Lv, X. Zhang, D. Wang, P. Li and S. Hui, *Appl. Therm. Eng.*, **154**, 485 (2019).
23. Y. Lu, Y. Wang, Y. Xu, Y. Li, W. Hao and Y. Zhang, *Appl. Therm. Eng.*, **121**, 224 (2017).
24. T. Chae, J. Lee, W. Yang and C. Ryu, *J. Mech. Sci. Technol.*, **30**, 3861 (2016).
25. M. Choi, X. Li, K. Kim, Y. Sung and G. Choi, *J. Mech. Sci. Technol.*, **32**, 4517 (2018).
26. X. Wang, Z. U. Rahman, Lv. Zhaomin, Y. Zhu, R. Ruan, S. Deng, L. Zhang and H. Tan, *Agronomy*, **11**, 810 (2021).
27. M. Öhman, D. Boström, A. Nordin and H. Hedman. *Energy Fuels*, **18**, 1370 (2004).
28. J. Morris, *Mechanisms and mitigation of agglomeration during fluidized bed combustion of biomass*, PhD Thesis (2021).
29. H. Wu, P. Glarborg, F. J. Frandsen, K. Dam-Johansen, P. A. Jensen and B. Sander, *Fuel*, **90**, 1980 (2011).
30. P. Plaza, *The development of a slagging and fouling predictive methodology for large scale pulverised boilers fired with coal/biomass blends*, PhD Thesis (2013).
31. H. Wu, A. J. Pedersen, P. Glarborg, F. J. Frandsen, K. Dam-Johansen and B. Sander, *Proc. Combust. Inst.*, **33**, 2845 (2011).
32. Y. Wang, X. Li and J. O. L. Wendt, *Energy Fuels*, **32**, 4391 (2018).
33. B.-H. Lee, S.-I. Kim, S.-M. Kim, D.-H. Oh, S. Gupta and C.-H. Jeon, *Korean J. Chem. Eng.*, **33**, 147 (2016).
34. C. Liu, Z. Liu, T. Zhang, X. Huang, J. Guo and C. Zheng, *Energy Fuels*, **31**, 2596 (2017).
35. E. Lindström, M. Sandström, D. Boström and M. Öhman, *Energy Fuels*, **21**, 710 (2007).